

Advances in the characterization of rough fractures in hydrocarbon reservoirs

Steven Ogilvie¹, Evgeny Isakov & Paul Glover

Introduction

A multitude of factors control the flow of fluids through fracture systems in hydrocarbon reservoirs. For example, closed fractures i.e. (deformation bands) may seal or baffle hydrocarbon flow (Fossen & Hesthammer 1998) whereas open fractures are considered to be conductive to hydrocarbon flow. However, fracture surface roughness has much control upon fluid flow through open fractures and is demonstrated to effect significant departures from the Cubic Law for predicting flow through fracture apertures (Isakov *et al.* 2001a). Such considerations are crucial in igneous and metamorphic reservoir rocks since fractures in these rocks may form the only significant pathways for fluid migration (Isakov *et al.* 2001b) (Fig. 1).

We present a five-stage approach for the full characterization of rough fracture surfaces in rocks and their incorporation into reservoir flow models. Each stage is aided by in-house developed software (Fig. 2).

- 1 Optical profiling of resin replicas of rough fracture surfaces in a suite of rocks (Fig. 2), using OPTPROF (Isakov *et al.* 2001a; Ogilvie *et al.* 2001a),
- 2 Parameterization and statistical analysis of the surfaces using PARAFAC software (Isakov *et al.* 2001c),
- 3 Creation of synthetic fractures tuned to the properties of the real rock fractures using SYNFR7AC software (Isakov *et al.* 2001c),

4 Experimental investigation of fluid flows (Ogilvie *et al.* 2001b).

5 Computational fluid flow modelling in 2D cross sections of fractures [boundary conditions from 1 to 4].

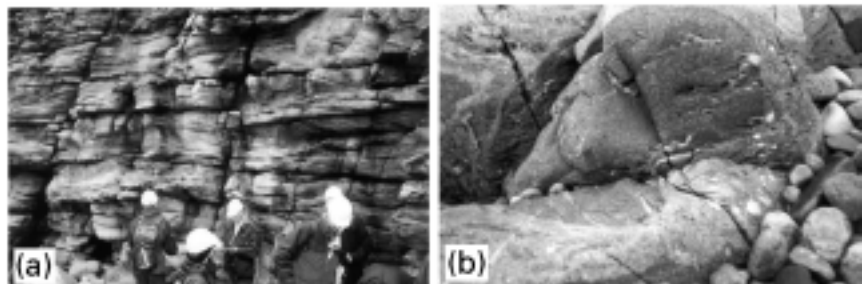
The objective is to replace the parallel-plate model assumed in larger multi-fracture models with a model that fully accounts for rough fractures at a range of scales.

1. Advances in optical profiling

A variety of rough fractures in crystalline and sedimentary rocks have been profiled using a fuller and more formalized optical method than previous attempts at utilisation of the Lambert-Beer Law (e.g. Yeo *et al.* 1998; Amundsen *et al.* 1999). It involves the creation of resin replicas of rough fracture surfaces and the imaging of them while covered with water and then dyed water. The digital optical imaging set-up consists of a high quality digital colour camera mounted on a frame directed towards a light box (Fig. 3). The camera gives a high lateral resolution of 15–200 μm for imaged areas of $7.5 \times 10 \text{ mm}$ and $100 \times 133 \text{ mm}$, respectively, and a similar vertical resolution. The digital video capture device is used to accurately measure the intensity of light across the camera view field.

The advances in optical imaging are documented in Isakov *et al.* (2001a) and in Ogilvie *et al.* (2001a) and include: (i)

Figure 1 (a). Highly fractured Upper Devonian Sandstones, Caithness, Scotland. (b) Fractured Dalradian contact migmatites, Aberdeen, Scotland (field of view = 1 m across). Roughness has a large impact upon fluid flow through these fractures, however, in (b) flow mainly occurs in the fracture network.



¹Department of Geology & Petroleum Geology, Meston Building, Kings College, University of Aberdeen, Aberdeen, AB24 3UE. E-mail: s.ogilvie@abdn.ac.uk, URL: Petrophysics.webhop.net

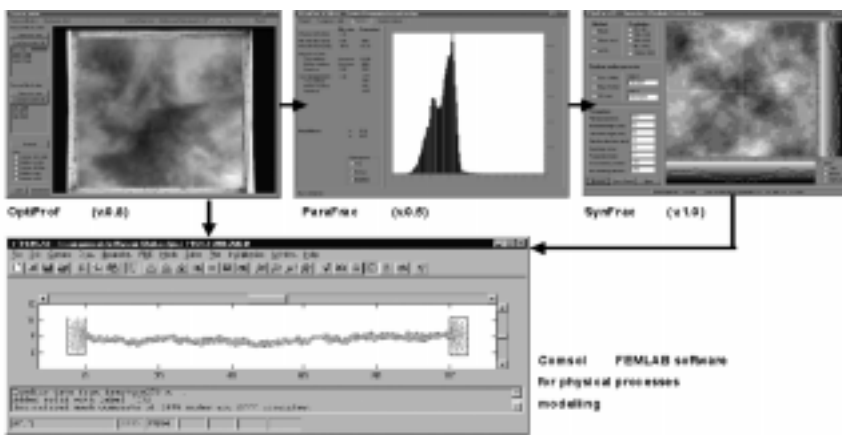


Figure 2 The software framework for the full characterization of rough fractures in rocks. OPTIPROF provides considerable control over the imaging process and calculates the final surface topographies. This data can be input into FEMLAB physical process modelling software. Input also comes from numerical models created using PARAFRAC and SYNFRAC software, which are tuned to the profiling data.

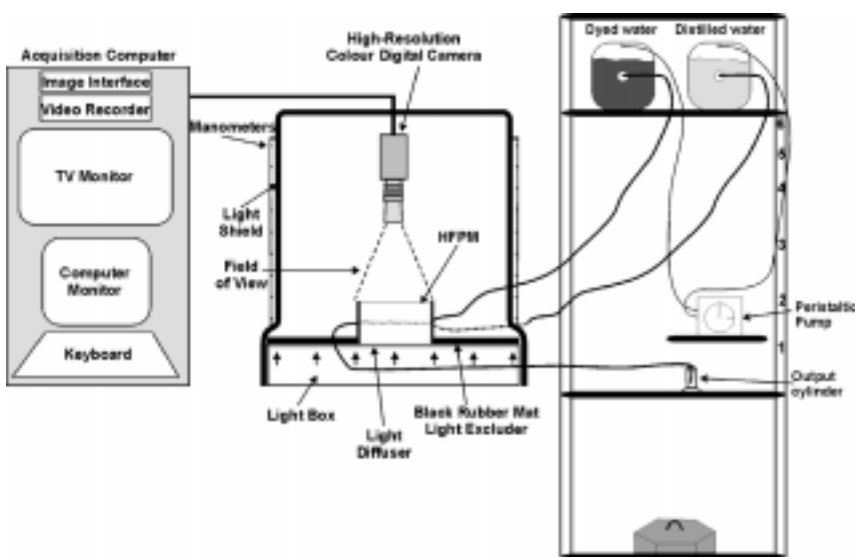


Figure 3 Digital optical imaging setup for (i) point-wise determination of fracture aperture, and (ii) the tracking of fluid flow through rough fractures (Fig. 9).

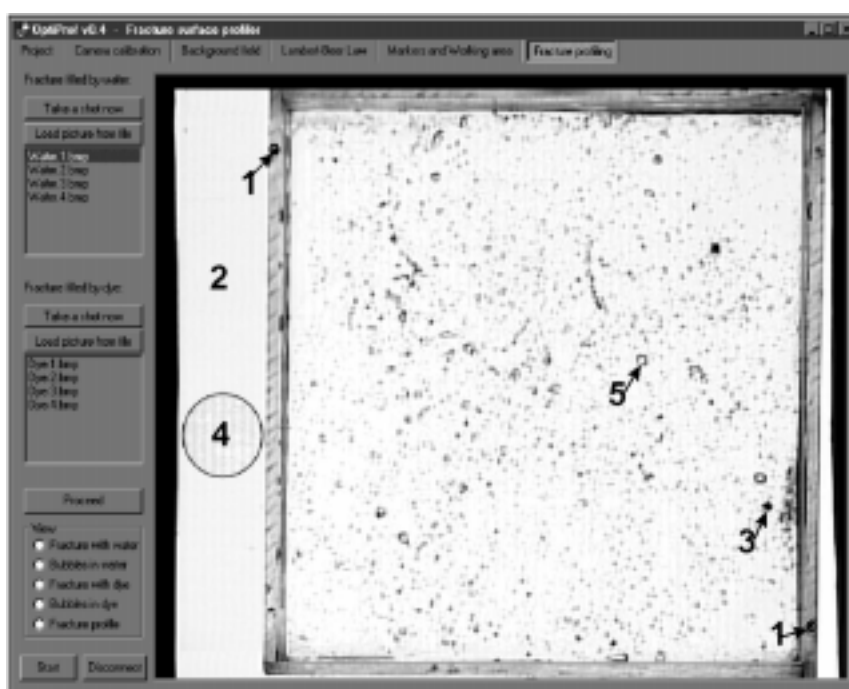


Figure 4 An image of the HPPM during measurement by fracture surface profiler software (OptiProf) showing the different technical difficulties encountered and their solutions: (1) Usage of location marks on walls to lock HPPM in position during imaging. (2) Dynamic noise across whole image is removed by image stacking techniques. (3) Particles in the HPPMs (4) Static distortions giving regular structure in video signal are removed using an attenuator connected to the video capture board. (5) Bubbles and dust in fluids are recognized as objects which move and are removed.

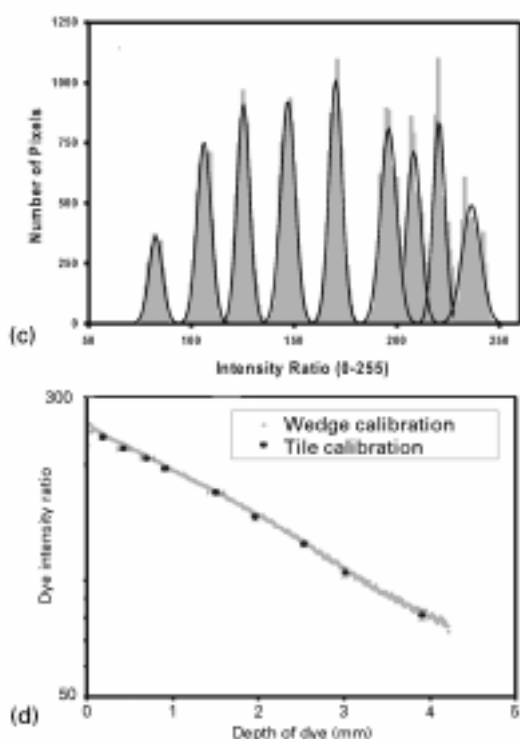
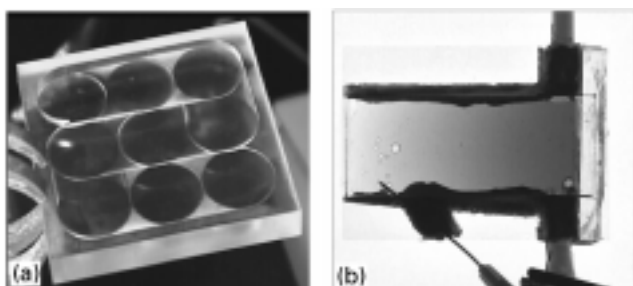


Figure 5 Robust methodologies for calibrating the measuring equipment, when dyed water of 1 g/L is used. (a) Polycarbonate tile device with nine pockets of known thickness (b) secondary wedge device with thickness variation from 0 on the left to 4.3 mm on the right (c) individual pockets of the tile analysed for intensity distributions (d) ratio of intensity of images for HFPMs containing dye to those containing water against depth of dye. The errors in this data are well constrained by the scatter in the wedge data.

very high resolution of reproduction of high fidelity polymer models (HFPMs) i.e. to 1 μm , (ii) inclusion of image improvement and noise suppression features in OPTIPROF™ software (Fig. 4), which also calculates the final measured topography of the surface by calibrating the image produced to dye thickness, (iii) improvements in firmware image capture, and (iv) development of robust methodologies for calibrating the optical measurement equipment (Fig. 5) used in imaging.

The images of individual fracture surfaces are then proc-

essed using the data from (iv) to provide a map of the fluid thickness above the rough surface topography. The resulting data can be transformed to provide a fully determined topography for each surface and the data for two surfaces can be combined to provide an aperture map for the fracture where the surface touch at a single point or any greater mean aperture (Fig. 6). Laboratory-induced Mode I fracture surfaces in a syenite are presented in Fig. 6a and from a very durable sandstone in Fig. 6b with their respective optical profiles.

2–3. Creation of numerical models

We could carry out flow modelling on data from the natural fracture. However, profiling and analysing a natural fracture is expensive and time consuming, and ultimately we only have fluid modelling data from a single fracture that might not be representative of all such fractures in the rock. Synthetic fractures are quick and easy to create using SYNFRAC software (Figs 2, 6), and once the initial parameters are known (e.g. surface and aperture fracture dimensions, surface asperity height distributions, anisotropies, and matching characteristics) any number of different fractures with the same properties may be created. Flow modelling on a suite of such fractures allows the mean flow behaviour to be judged, which is representative of that type of fracture enabling us to recognize and account for particular topographic geometries, which may be unrepresentative of the suite in general.

Fundamental to this procedure is choice of appropriate fracture matching approach, i.e. once the surfaces are separated for profiling it is very difficult to match them together again for modelling purposes (Hakimi & Larsson 1996). In the classic Brown (1995) model the Mismatch Length (ML) represents the wavelength lower than which there is no correlation between the two fracture surfaces and higher than which there is complete matching (Fig. 7a). However this model is not mathematically robust and essentially underestimates the fracture aperture, while the improved Glover *et al.* (1998a) model slightly overestimates it (Fig. 7b). Our new definition provides more flexibility and recognizes that the development of matching behaviour is more complex, and the new definition is a measure of the wavelength half way between the largest wavelength at which minimum matching occurs and the smallest wavelength at which maximum matching occurs. The following are introduced for the Glover *et al.* (1998a, 1998b) and our new improved method to enable more flexibility in modelling (Fig. 7c):

- Maximum Matching Fraction (MaxMF), which is a maximum value of matching, expressed as a fraction of complete matching, that is defined at the largest wavelength of the HFPM.
- Minimum Matching Fraction (MinMF), which is a minimum value of matching
- Transition length (TL), which describes how fast in

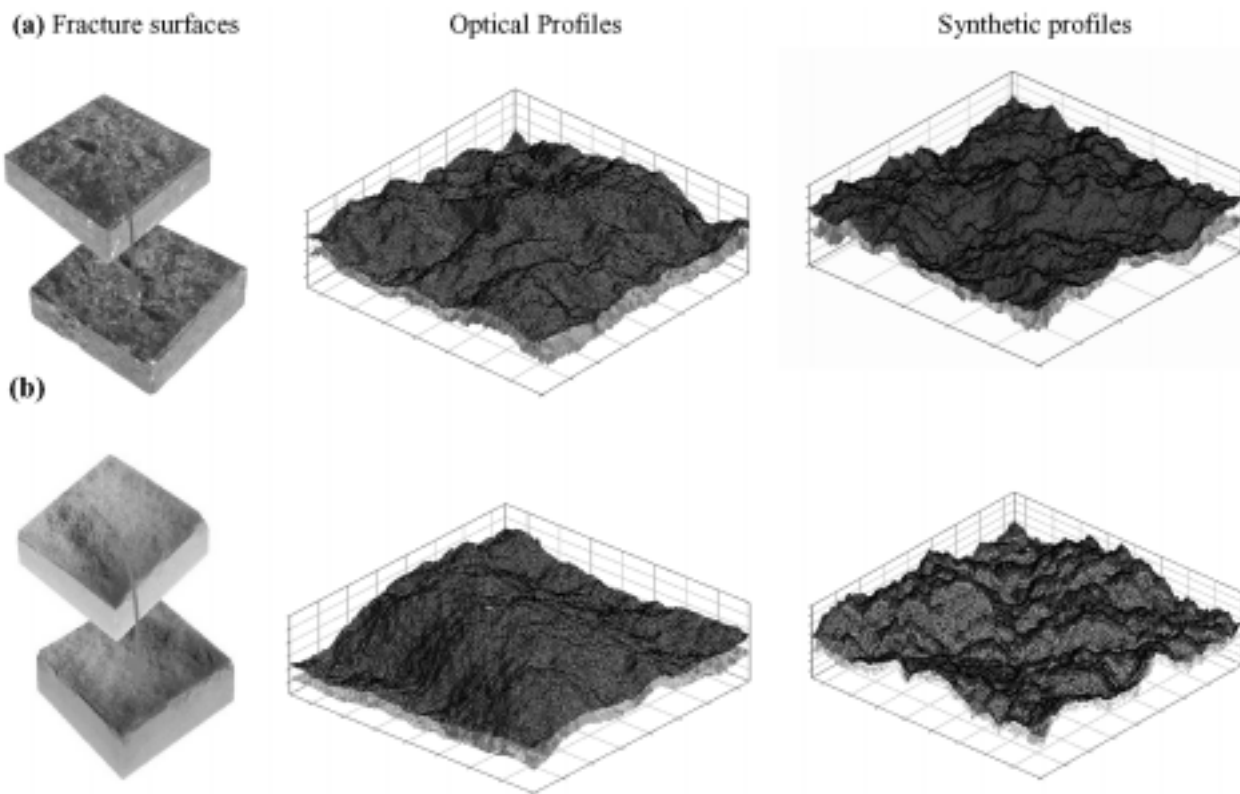


Figure 6 Laboratory induced Mode I fractures in (a) syenite (Norway) and (b) sandstone (Clashach Sandstone, NE Scotland) with respective optical and synthetic profiles.

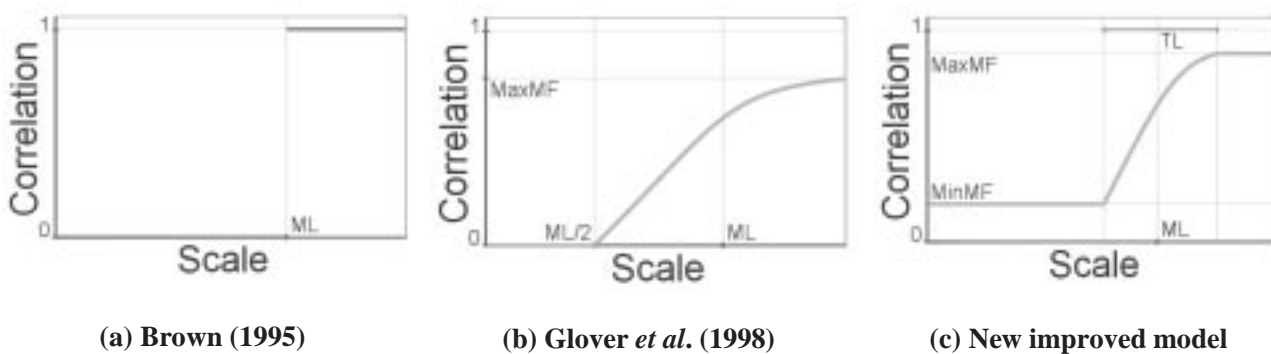


Figure 7 Approaches in the matching of fracture surfaces. (a) the classic approach used by Brown (1995) (b) the approach used by Glover *et al.* (1998a,b), and (c) the new, improved approach to more accurately reflect matching behaviour in natural fractures.

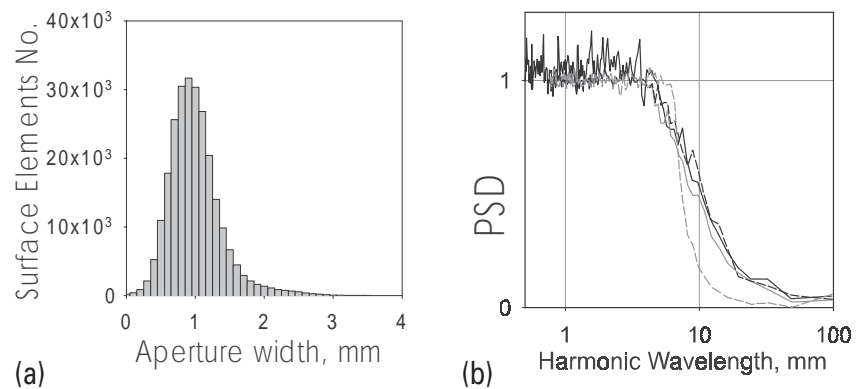
wavelength (or wavenumber) space the matching develops i.e. it is the difference in wavelength between that at which maximum matching occurs and that at which minimum matching occurs.

These are implemented as a software algorithm in SYNFRAC.

The fractures studied have an aperture with approximate

gaussian distributions of elevation of surface elements (Fig. 8a). The power spectral densities (PSD) ratios (Fig. 8b) show that the Glover *et al.* (1998a,b) model and our new model more closely reflect the matching properties of real rock fractures than the Brown (1995) approach and are therefore better predictors of fracture apertures in rough fractures.

Figure 8 Fracture parameterization and statistical analysis (a) All apertures approximate Gaussian distributions. (b) Power spectral density (PSD) ratio plots for derivation of fracture parameters of syenite. Natural fracture (—), AUPG model (---), Glover *et al.* model (—), Brown model (---).



4-5. Single-phase fluid flow experimentation and modelling

A combined experimental–modelling approach enables the physical constraints upon fluid flow through rough fractures to be well characterized (Ogilvie *et al.* 2001b). The high fidelity polymer models (HFPMs) are mated and inserted into a flow cell (Fig. 9) which has input/output ports and flow manifolds to receive and distribute the fluids evenly across the fracture at controlled rates and pressures. Higher concentrations of dyed water (5 g/L) are used than for the point-wise determination of aperture to aid flow visualization. Carbon dioxide is released into the water filled HFPMs from CO₂ sparklets to push air bubbles out of the HFPMs. The remaining CO₂ effectively dissolves in the water. The digital optical imaging setup (Fig. 3) is linked to water and dyed water fluid reservoirs and a gravity-driven flow frame. The output is moved from position 1–6 on the gravity-driven flow setup and flow rate, Q , vs. pressure head, ΔP , recorded at each stage using manometers. The HFPMs are wetted using water and dyed water is released from its reservoir to push water out of the HFPM at high flow rates. At lower flow rates a peristaltic pump is used (Fig. 3); the manometers dampen any fluid pulsing.

Image analysed fluid flow fronts of dyed water through an HFPM of syenite are illustrated in Figs 10(a, c) for Reynold’s numbers of 1.2 and 12.6, respectively, where, $Re = 1.5 Q/W\eta$ (Q = Flow charge (cm³/s), W = Width of aperture, η = kinematic viscosity). The flow fronts are separated from the background by performing a Clearfield equalization, using the first frame as the Clearfield and are image analysed into intensity bins. The flow modelling was carried out in a FEMLAB environment. The Reynold’s Numbers from the 2D FEMLAB flow simulations are prescribed to fit those of the experiments and the profiling data (image analysed topographies) also provides physical boundary input into the FEMLAB models (Figs 2, 10b,d). The flow scales for the simulations show rela-

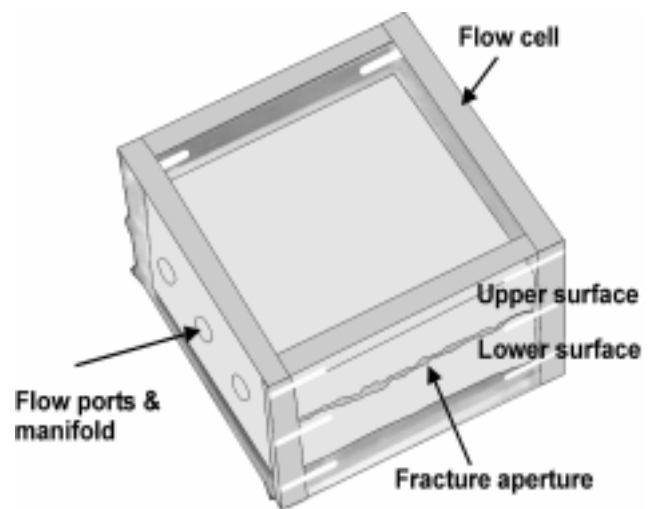


Figure 9 Flow cell containing HFPMs for fluid flow experiments.

tive concentrations of dye where the top = high and the bottom = undyed water.

It is clear that the fluid front (along modelling profile in Figs 10a,c) reaches the output end of the aperture at the same time as the equivalent simulation frame. Also, dye intensities decrease at the head of flow fronts indicating that less aperture is filled at the output end of the fracture. The $Re = 12.6$ images show more jet-type behaviour as there is less time to distribute the fluid from the input pipes over the fracture surface. Furthermore, the equivalent time frames in $Re = 1.2$ are approximately 12 times longer than those in $Re = 12.6$.

We introduce the dual mean for calculation of hydraulic aperture. The geometric mean is popularly used (Renshaw 1995) but collapses to 0 if any touching point exists in the aperture. The dual mean, a combination of arithmetic and

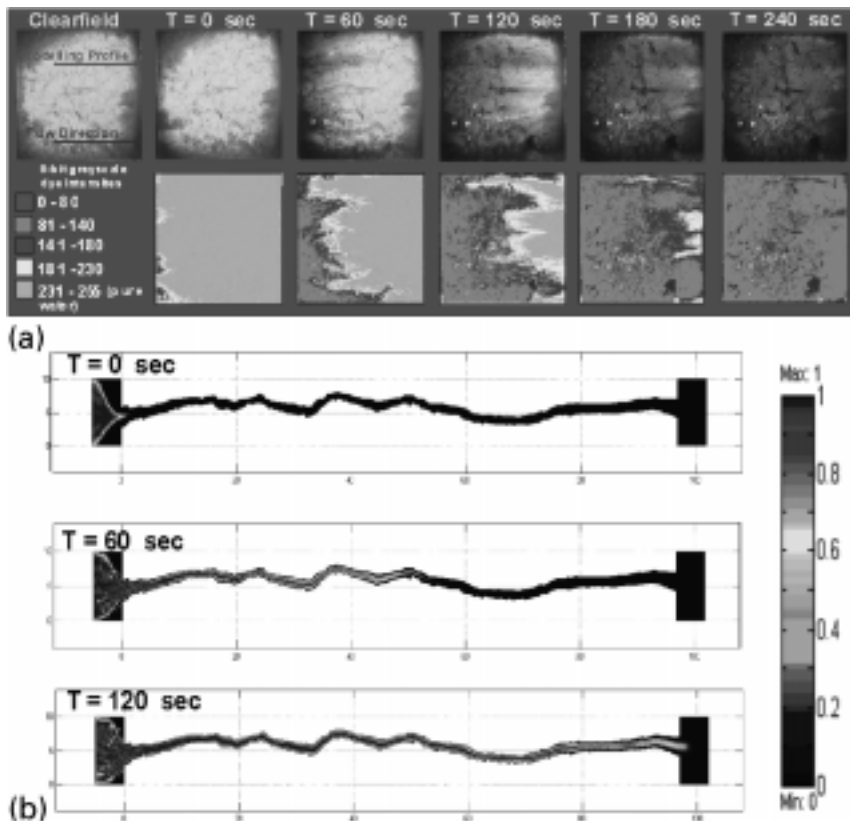


Figure 10 A combined experimental-modelling approach for the tracking of fluid flow through rough fractures. (a) Experimental fluid flow through an HFPM of syenite for when $Re = 1.2$, Flow charge, $Q = 0.08 \text{ cm}^3$ and (b) respective simulations. (c) Experimental fluid flow for when $Re = 12.6$, Flow charge, $Q = 0.76 \text{ cm}^3$, and respective simulations (d).

geometric means has the advantages of (i) removing the difficulty of 0 calculated aperture for rock apertures that touch at a single point, and (ii) has different values for each flow direction and is therefore anisotropic.

Conclusions

Fracture surface roughness has been the subject of active research over the last decade showing that roughness (together with many other interrelated factors) has a large control upon the flow of fluids through fracture networks. Our combined experimental/modelling approach of rough fracture characterization is proving successful in our drive to replace the cubic-law with a model that fully accounts for roughness at a range of scales. This is aided by in-house developed software, OPTIPROF, PARAFRAC and SYNFRAC which have easy to understand GUIs and are written in C++ to be run on PC computers under Windows 95/98/NT operating systems. These are freely available to download from our website at <<http://petrophysics.webhop.net>>.

The following issues are currently being addressed:

- The creation and modelling of Mode II and III (shearing) fractures by adding shearing options to SYNFRAC.
- The scaling behaviour of rough fractures by zooming into

smaller areas of each HFPM and performing comparative statistical analyses.

References

Amundsen, H. Wagner, W. Oxaal, U. Meakin, P. Feder and J. Jossang, T. [1999] Slow-two-phase flow in artificial fractures: Experiments and simulations. *Water Resources Research* 35, 2619–2626.

Brown, S.R. [1995] Simple mathematical model of a rough fracture. *Journal of Geophysical Research* 91, 5941–5952.

Fossen, H. and Hesthammer, J. [1998] Deformation bands and their significance in porous sandstone reservoirs. Research article. *First Break* 16(1), 21–25.

Glover, P.W.J., Matsuki, K., Hikima, R. and Hayashi, K. [1998a] Synthetic rough fractures in rocks. *Journal of Geophysical Research* 103, 9606–9620.

Glover, P.W.J., Matsuki, K., Hikima, R. and Hayashi, K. [1998b] Fluid flow in synthetic rough fractures and application to the Hachimantai geothermal HDR test site. *Journal of Geophysical Research* 103, 9621–9635.

Hakimi, E. and Larsson, E. [1996] Aperture measurements and flow experiments on a single natural fracture. *International Journal of Rock Mechanics and Mineral Science Abstracts* 33, 395–404.

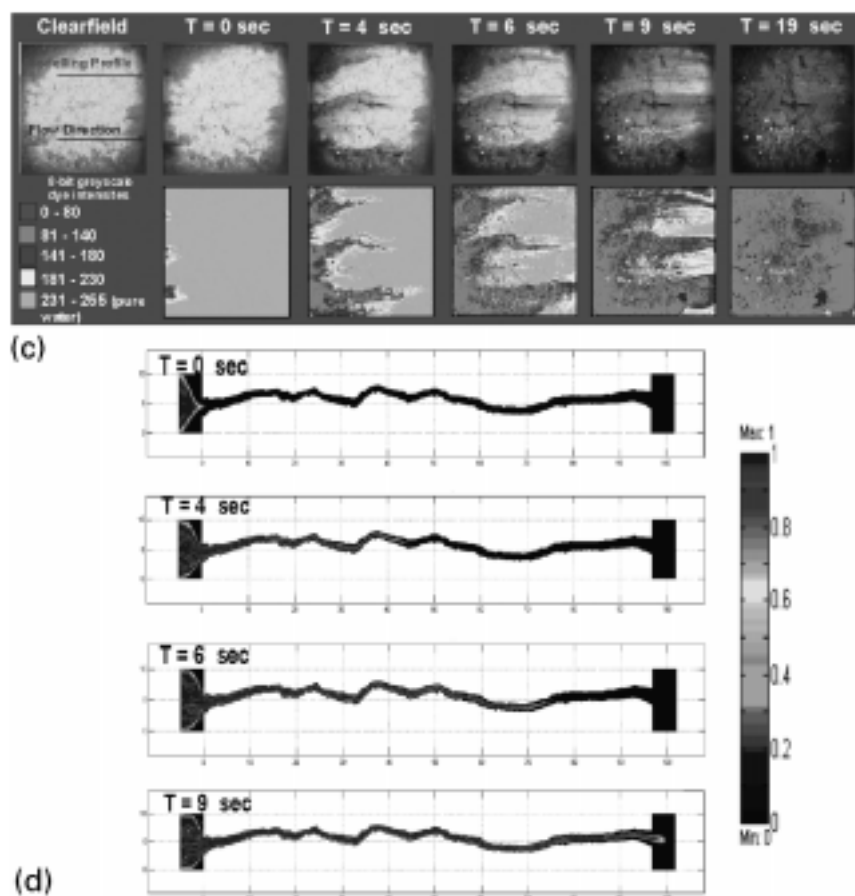


Figure 10 Continued.

Isakov, E., Glover, P.W.J. and Ogilvie, S.R. [2001c] Use of synthetic fractures in the analysis of natural fracture apertures. *Proceedings of the 8th European Congress for Stereology and Image Analysis, Image Analysis and Stereology* 20(2) Suppl. 1, September, 366–371.

Isakov, E., Ogilvie, S.R. and Glover, P.W.J. [2001b] High-resolution aperture determinations of rough fractures in crystalline rocks. *Hydrocarbons in crystalline rocks*, Meeting of Geology Society of London, 13–14 February.

Isakov, E., Ogilvie, S.R., Taylor, C.W. and Glover, P.W.J. [2001a] Fluid flow through rough fractures in rocks i: high resolution aperture determinations. *Earth and Planetary Science Letters* 191(3–4), 267–282.

Ogilvie, S.R., Isakov, E., Glover, P.W.J. and Taylor, C.W. [2001a] A new high resolution optical method for obtaining the topography of fracture surfaces in rocks. *Proceedings of the 8th European Congress for Stereology and Image Analysis, Image Analysis and Stereology* 20(2) Suppl. 1, September, 386–391.

Ogilvie, S.R., Isakov, E., Glover, P.W.J. and Taylor, C.W. [2001b] Use of image analysis and finite element analysis to characterise fluid flow in rough rock fractures and their synthetic analogues. *Proceedings of the 8th European Congress for Stereology and Image Analysis, Image Analysis and Stereology* 20(2) Suppl. 1, September, 504–509.

Renshaw, C.E. [1995] On the relationship between mechanical and hydraulic apertures in rough-walled fractures. *Journal of Geophysical Research* 100, 24629–24636.

Yeo, I.W., De Freitas, M.H. and Zimmerman, R.W. [1998] Effect of shear displacement on the aperture and permeability of a rock fracture. *International Journal of Rock Mechanics and Mineral Science Abstracts* 35, 1051–1070.